Geomechanics and Engineering, *Vol. 7, No. 3 (2014) 263-277*
DOI: http://dx.doi.org/10.12989/gae.2014.7.3.263

Effect of seismic acceleration directions on dynamic earth pressures in retaining structures

Ting-Kai Nian [*1,2], Bo Liu [1], Jie Han [3] and Run-Qiu Huang [2]

[1] *School of Civil Engineering & State Key Laboratory of Coastal and Offshore Engineering, Dalian University of Technology, Dalian 116024, China*
[2] *State Key Laboratory of Geohazard Prevention and Geoenvironmental Protection, Chengdu University of Technology, Chengdu 610059, China*
[3] *Department of Civil, Environmental and Architectural Engineering, the University of Kansas, Lawrence, KS 66045, USA*

(*Received February 24, 2013, Revised April 22, 2014, Accepted May 16, 2014*)

Abstract. In the conventional design of retaining structures in a seismic zone, seismic inertia forces are commonly assumed to act upwards and towards the wall facing to cause a maximum active thrust or act upwards and towards the backfill to cause a minimum passive resistance. However, under certain circumstances this design approach might underestimate the dynamic active thrust or overestimate the dynamic passive resistance acting on a rigid retaining structure. In this study, a new analytical method for dynamic active and passive forces in c-ϕ soils with an infinite slope was proposed based on the Rankine earth pressure theory and the Mohr-Coulomb yield criterion, to investigate the influence of seismic inertia force directions on the total active and passive forces. Four combinations of seismic acceleration with both vertical (upwards or downwards) and horizontal (towards the wall or backfill) directions, were considered. A series of dimensionless dynamic active and passive force charts were developed to evaluate the key influence factors, such as backfill inclination β, dimensionless cohesion $c/\gamma H$, friction angle ϕ, horizontal and vertical seismic coefficients, k_h and k_v. A comparative study shows that a combination of downward and towards-the-wall seismic inertia forces causes a maximum active thrust while a combination of upward and towards-the-wall seismic inertia forces causes a minimum passive resistance. This finding is recommended for use in the design of retaining structures in a seismic zone.

Keywords: earth pressure; retaining structures; analytical solution; horizontal and vertical seismic coefficients

1. Introduction

The failures of retaining structures as earth retaining walls and stabilizing piles against sliding under seismic loading have been reported by several researchers (Seed and Whitman 1970, Wood 1973, Fang and Chen 1995, Ling and Leshchinsky 1998, Das 2008). Recently, Yao *et al*. (2009) investigated the failure of retaining structures adjacent to slopes after the magnitude 8.0 Wenchuan Earthquake of China in 2008. They compiled different modes of earthquake-induced failures of retaining structures, which include large inclination of stabilizing piles, dislocation, outward

*Corresponding author, Associate Professor, E-mail: tknian@dlut.edu.cn

http://www.techno-press.org/?journal=gae&subpage=7 ISSN: 2005-307X (Print), 2092-6219 (Online)

deformation, overall failure of mortar stone facing retaining walls, mid-height shear failure or horizontal sliding at the bottom of concrete retaining walls, embankment failure due to the overturning of retaining walls, and global failure of reinforced earth retaining walls, etc. Sliding and overturning of retaining structures are two common failure modes observed after an earthquake, which result from the increase of lateral earth pressure. Clearly, dynamic earth pressure is an important parameter for controlling the stability of earth retaining structures in a seismic zone.

Currently, two earth pressure theories are widely adopted to calculate the dynamic earth pressures in earth retaining structures, which are based on the Coulomb sliding wedge concept (Mononobe 1924, Okabe 1924, Kapila 1962, Seed and Whitman 1970, Fang and Chen 1995, Choudhury and Nimbalkar 2005, Ghosh 2008, Shukla *et al*. 2009, Shukla and Habibi 2011) and the Rankine limit stress state (Richards *et al*. 1990, Budhu and Al-Karni 1993, Richards and Shi 1994, Lancellotta 2002 and 2007). The past studies have investigated cohesionless and c-ϕ backfill (c is cohesion and ϕ is friction angle) with, horizontal and inclined ground surfaces, and under horizontal and vertical seismic loading conditions. However, the direction effect of horizontal and vertical seismic inertia forces and seismic earth pressures on retaining structures under a combination of horizontal (towards the wall or backfill) and vertical (upward or downward) seismic inertia forces have not been well studied (Fang and Chen 1995, Shukla and Habibi 2011). In the conventional design, a combination of upward and towards-the-wall seismic inertial forces is assumed to cause a maximum active thrust (Mononobe 1924, Okabe 1924, Fang and Chen 1995), while a combination of upward and towards-the-backfill seismic inertial forces is assumed to cause a minimum passive resistance (Kapila 1962, Fang and Chen 1995, Shukla and Habibi 2011). Nian and Han (2013) investigated the seismic active earth pressure in c-ϕ soil with an infinite slope. In fact, it is not clear under which combination of the seismic loading directions the retaining structure is in the most dangerous state of instability and how to properly consider this critical state in the design of retaining structures in a seismic zone. To the authors' knowledge, under certain circumstances the conventional design in which seismic inertia forces act upwards and towards the wall (i.e., an active state), may underestimate the seismic active thrust while it may overestimate the seismic passive resistance when the seismic inertia forces act upwards and towards the backfill (i.e., a passive state). In the present study, the analytical solutions for seismic lateral earth pressure/force were obtained based on the Rankine earth pressure theory, and then they are used to investigate the influence of the seismic acceleration directions on active and passive forces acting on earth retaining structures in a seismic active zone.

2. Analytical formulation

Fig. 1(a) shows a typical soil slice ABCD with a height z and a unit width 1 in an infinite slope with an angle β. The base of the soil slice is parallel to the slope surface. The effect of the left-side soil mass of the cross section (i.e., AB) in the infinite slope can be replaced by a rigid retaining structure such as a retaining wall or a row of stabilizing piles against sliding, which is rather common in practice. In this study, the AB surface is assumed to be vertical and smooth. In a limit equilibrium state under self-weight and seismic inertia forces in the semi-infinite mass of the c-ϕ soil, the inclined lateral pressure value at the interface AB is the seismic active or passive earth pressure acting on a retaining structure of cohesive backfill with an infinite top slope. Herein, the

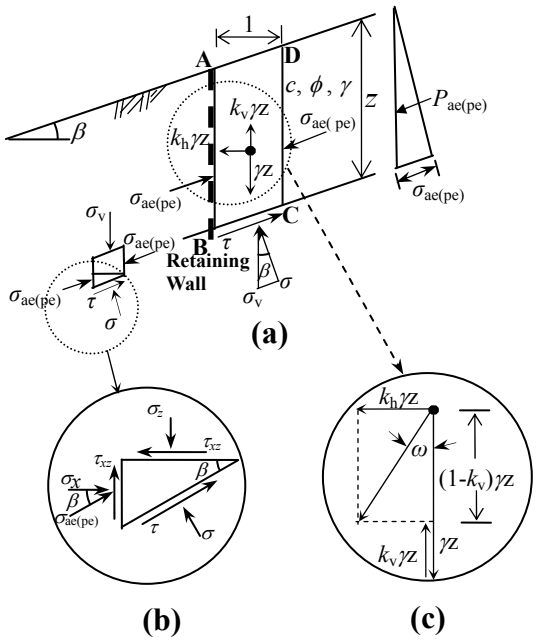

Fig. 1 Force analysis of the soil slice in an infinite slopes under seismic loading: (a) Forces on the soil slice; (b) Stresses on the wedge element; (c) Definition of the direction angle ω induced by horizontal and vertical seismic inertia forces (Modified from Nian and Han 2013)

seismic active or passive earth pressure on the retaining wall is assumed to be parallel to the inclined backfill surface.

Prior to the stress analysis, the following assumptions were made:

(1) the soil-wall interface is vertical and smooth;
(2) the backfill is cohesionless or c-ϕ soil;
(3) the ground surface is horizontal or inclined;
(4) the self-weight of the soil slice is γz, where γ is the unit weight of the soil;
(5) the seismic inertia forces on the soil slice are horizontal (towards the wall facing or backfill) and vertical (upwards or downwards), i.e., $k_h\ \gamma z$ [←+/→–] and $k_v\ \gamma z$ [↓+/↑–], where k_h and k_v are the horizontal and vertical seismic coefficients respectively;
(6) the seismic direction angle ω of horizontal and vertical seismic inertia forces is defined as $\omega = \tan^{-1}\left(\frac{\pm k_h}{1 \pm k_v}\right)$, in which the positive sign "+" and the negative sign "–" before the term k_v indicate that the seismic inertia forces act downwards and upwards, respectively while the positive sign "+" and the negative sign "–" before the term k_h indicate that the seismic inertia forces act towards the wall facing and the backfill, respectively (Figs. 1(a) and (c)).

The normal stress σ and shear stresses τ obtained from the force equilibrium can be substituted

into those from the wedge stress analysis to obtain the vertical stress σ_z and shear stress τ_{xz} which satisfy the equilibrium and are expressed by a combination of the parameters: σ_x, γz, $1 \pm k_v$, $\tan\beta$ and $\tan\omega$ (σ_x is an unknown variable). Furthermore, the vertical stress σ_z and shear stress τ_{xz} can be substituted into the following relationship to obtain the major and minor principal stresses (Nian and Han 2013)

$$\begin{pmatrix}\sigma_1\\ \sigma_3\end{pmatrix}=\frac{1}{2}(\sigma_z+\sigma_x)\pm\sqrt{\left[\frac{1}{2}(\sigma_z-\sigma_x)\right]^2+\tau_{xz}^2} \tag{1}$$

These principal stresses (σ_1, σ_3) are a function of σ_x and satisfy both the equilibrium within the soil domain of the slope and the stress boundary conditions. According to the lower-bound limit analysis concept (Chen 2007), this stress field (σ_1, σ_3) is statically allowable if it nowhere violates the yield condition, such as the Mohr-Coulomb criterion. When the principal stresses (σ_1, σ_3) are substituted into the following Mohr-Coulomb failure criterion (Nian and Han 2013)

$$\frac{1}{2}(\sigma_1-\sigma_3)=\frac{1}{2}(\sigma_1+\sigma_3)\sin\phi+c\cos\phi \tag{2}$$

a quadratic equation as a function of σ_x can be obtained, in which c and ϕ are cohesion and friction angle of the soil, respectively. Solving this equation yields two principal values of the horizontal stress σ_x in a statically allowable stress field. The components $\sigma_x/\cos\beta$ are the seismic active and passive earth pressures (σ_{ae} and σ_{pe}) on the retaining wall of c-ϕ backfill with an infinite top slope as expressed below

$$\begin{pmatrix}\sigma_{\mathrm{pe}}\\ \sigma_{\mathrm{ae}}\end{pmatrix}=\frac{\sigma_x}{\cos\beta}=(1\pm k_{\mathrm{v}})\gamma z\cdot\cos\beta\left[J\pm\sqrt{J^2-(1+A)^2-\frac{4\tan^2\omega}{\cos^2\phi}+\frac{4D}{1\pm k_{\mathrm{v}}}\tan\phi(1+A)+\left(\frac{2D}{1\pm k_{\mathrm{v}}}\right)^2}\right] \tag{3a}$$

or

$$\begin{pmatrix}\sigma_{\mathrm{pe}}\\ \sigma_{\mathrm{ae}}\end{pmatrix}=\frac{\sigma_x}{\cos\beta}=(1\pm k_{\mathrm{v}})\gamma z\cdot K \tag{3b}$$

where

$$K=\begin{pmatrix}K_{\mathrm{pe}}\\ K_{\mathrm{ae}}\end{pmatrix}=\cos\beta\cdot\left[J\pm\sqrt{J^2-(1+A)^2-\frac{4\tan^2\omega}{\cos^2\phi}+\frac{4D}{1\pm k_{\mathrm{v}}}\tan\phi(1+A)+\left(\frac{2D}{1\pm k_{\mathrm{v}}}\right)^2}\right] \tag{3c}$$

$$J=(1+A)\left(\frac{2\cos^2\beta}{\cos^2\phi}\cdot\frac{1-A}{1+A}-1\right)+\frac{2D}{1\pm k_{\mathrm{v}}}\tan\phi \tag{3d}$$

$$A=\tan\beta\tan\omega,\quad D=\frac{c}{\gamma z},\quad z\neq 0 \tag{3e}$$

K is the seismic lateral pressure coefficient, K_{ae} and K_{pe} are the seismic active and passive earth

pressure coefficients, respectively, and the other parameters are defined earlier. The selection of "–" or "+" sign for the optional sign "±" before the square root in Eq. (3) implies the active or passive state of limit equilibrium. Especially, the analytical expressions of the seismic active and passive earth pressures (σ_{ae} and σ_{pe}) at $z = 0$ can be rewritten as

$$\begin{aligned}\begin{pmatrix}\sigma_{\mathrm{pe}}\\ \sigma_{\mathrm{ae}}\end{pmatrix} &= \frac{\sigma_x}{\cos\beta} = \left(2c\tan\phi \pm \sqrt{(2c\tan\phi)^2 + 4c^2}\right)\cos\beta \\ &= 2c\frac{\sin\phi \pm 1}{\cos\phi}\cos\beta\end{aligned} \tag{4}$$

To check the reasonableness of the analytical solution, a special case that has a cohesionless backfill with a horizontal ground surface under seismic loading is adopted, that is, $\beta = 0$, $c = 0$, $\phi \neq 0$, $k_h \neq 0$, and $k_v \neq 0$. Eq. (3c) can be reduced to the following equation since $\beta = 0$ and $c = 0$

$$K = \begin{pmatrix}K_{\mathrm{pe}}\\ K_{\mathrm{ae}}\end{pmatrix} = \frac{1+\sin^2\phi}{\cos^2\phi} \pm \frac{2}{\cos\phi}\sqrt{\tan^2\phi - \tan^2\omega} \tag{5a}$$

Eq. (5a) is the same as that presented by several investigators (Richards *et al*. 1990, Budhu and Al-Karni 1993, Richards and Shi 1994) using a graphic geometry procedure. Furthermore, if $k_h = 0$ and $k_v = 0$, Eq. (5a) can be reduced to

$$K = \begin{pmatrix}K_{\mathrm{pe}}\\ K_{\mathrm{ae}}\end{pmatrix} = \frac{(1\pm\sin\phi)^2}{(1+\sin\phi)(1-\sin\phi)} = \begin{pmatrix}K_{\mathrm{p}}\\ K_{\mathrm{a}}\end{pmatrix} \tag{5b}$$

Eq. (5b) is the classical Rankine earth pressure formula for a cohesionless soil with a horizontal ground surface (Terzaghi 1943, Gnanapragasam 2000), where K_a and K_p are respectively the active and passive earth pressure coefficients based on Rankine's theory as follows

$$K_{\mathrm{p}} = \frac{1+\sin\phi}{1-\sin\phi}, \quad K_{\mathrm{a}} = \frac{1-\sin\phi}{1+\sin\phi} \tag{5c}$$

3. Distribution of seismic earth pressure

To investigate the distribution of seismic earth pressure, a design example is presented herein. Consider a rigid retaining wall is constructed to support a c-ϕ soil with an infinite top slope in a seismically active zone. The material properties and seismic parameters are listed in Table 1.

Table 1 Material properties and seismic parameters for a selected earth retaining structure

γ (kN·m^{-3})	c (kPa)	ϕ (°)	H (m)	β (°)	k_h (←)	k_v (↑)
Unit weight of soil	Cohesion of soil	Internal friction angle of soil	Height of retaining wall	Slope angle	Horizontal seismic coefficient	Vertical seismic coefficient
18.0	21.6	35	12	10	0.2	0.1

Calculations were performed using Eq. (3) to obtain the seismic active and passive earth pressures under horizontal and vertical seismic loading. The distributions of the seismic active and passive earth pressures along the wall height under upward and toward-the-wall seismic inertia force are shown in Fig. 2. Fig. 2 (a) shows that the seismic active earth pressure had a triangular distribution, and a tension crack zone (i.e., the negative seismic active earth pressure) existed within a critical depth z_c from the top of the retaining wall. However, it can be shown from Fig. 2 (b) that the seismic passive earth pressure shows a trapezoidal distribution.

4. Parametric study under seismic active condition

Fig. 2(a) shows a triangular seismic active earth pressure distribution with a tension crack

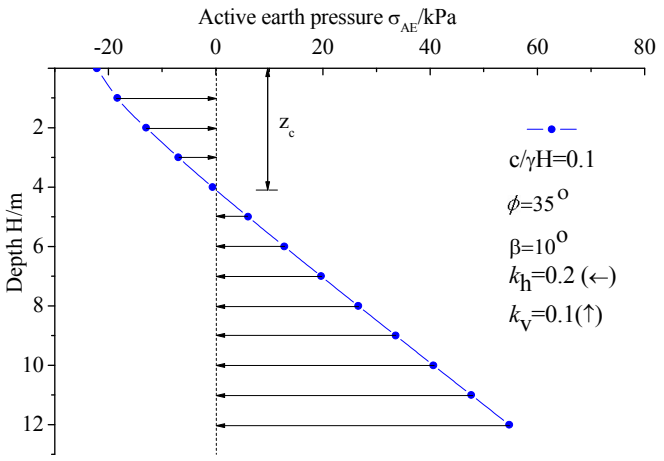

(a) Active condition

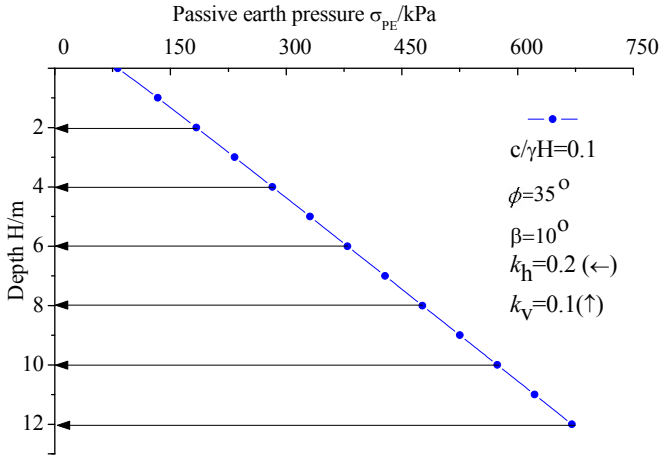

(b) Passive condition

Fig. 2 Distributions of seismic active and passive earth pressures at the depth from the top of the wall

within the range of critical depth z_c. The critical depth z_c can be obtained when the seismic active pressure $\sigma_{ae}=0$. Setting $\sigma_{\mathrm{ae}}=\dfrac{\sigma_x}{\cos\beta}=0$ in Eq. (3a) with some rearrangements results in a quadratic equation as follows

$$\left[(1+A)^2+\frac{4\tan^2\omega}{\cos^2\phi}\right]\cdot z^2-\frac{4(1+A)H\left(\dfrac{c}{\gamma H}\right)\tan\phi}{1\pm k_{\mathrm{v}}}\cdot z-\frac{4H^2\left(\dfrac{c}{\gamma H}\right)^2}{(1\pm k_{\mathrm{v}})^2}=0 \tag{6}$$

By solving Eq. (6), the critical depth z_c of the tension crack can be obtained (Nian and Han 2013)

$$z_{\mathrm{c}}=\frac{2H\left(\dfrac{c}{\gamma H}\right)}{\left[(1+A)^2+\dfrac{4\tan^2\omega}{\cos^2\phi}\right](1\pm k_{\mathrm{v}})\cos\phi}\cdot\left[\sin\phi(1+A)+\sqrt{(1+A)^2+4\tan^2\omega}\right] \tag{7}$$

Combined with Eq. (3), the active force P_{ae} acting on the retaining wall per unit length can be expressed as follows (Nian and Han 2013)

$$P_{\mathrm{ae}}=\frac{1}{2}\sigma_{\mathrm{ae}}\big|_{z=H}(H-z_{\mathrm{c}})=\frac{1}{2}K_{\mathrm{ae}}\big|_{z=H}(1\pm k_{\mathrm{v}})\gamma H(H-z_{\mathrm{c}}) \tag{8}$$

Eq. (8) can be reformatted in a dimensionless form below (Nian and Han 2013)

$$\overline{P_{\mathrm{ae}}}=P_{\mathrm{ae}}/(\tfrac{1}{2}\gamma H^2)=K_{\mathrm{ae}}\big|_{z=H}(1\pm k_{\mathrm{v}})\left(1-\frac{z_{\mathrm{c}}}{H}\right) \tag{9}$$

To investigate the influence of seismic acceleration directions on the seismic active force on a retaining wall, four combinations of seismic acceleration with the vertical (upwards or downwards) and horizontal (towards the wall or backfill) directions were adopted in the present analysis. The material parameters and seismic parameters used in this analysis are shown in Table 1. A series of dimensionless dynamic active forces were computed by changing the directions of horizontal and vertical seismic inertia forces, which are shown in Fig. 3.

Fig. 3 shows that the inertia force induced by the horizontal seismic acceleration towards the wall caused a higher active thrust than that towards the backfill, irrespective of the direction of the vertical seismic acceleration. This conclusion is also true for a case when only a horizontal seismic inertia force is applied, which is common in the retaining wall design. However, Fig. 3 shows that under a downward inertia force with a 0.2 g vertical acceleration, the seismic active thrust P_{ae} had a maximum value rather than that under an upward inertia force when the horizontal seismic acceleration was less than 0.35 g. From a practical viewpoint, a greater horizontal thrust P_{ae} implies a lower factor of safety against sliding and overturning. Therefore, a downward inertia force should be presented as the proposed approach, and be considered in the design of retaining structures unless under special circumstances such as a horizontal seismic acceleration higher than 0.35 g.

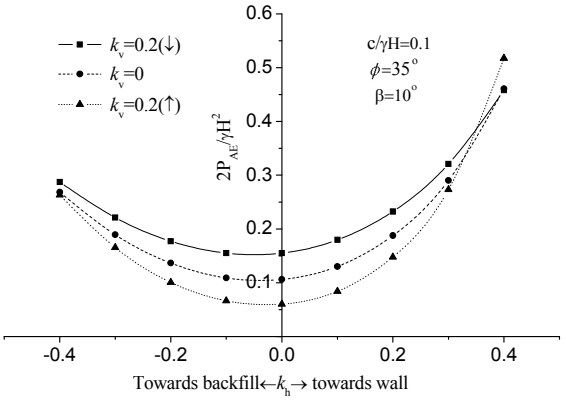

Fig. 3 Influence of the direction of inertia force on the seismic active thrust

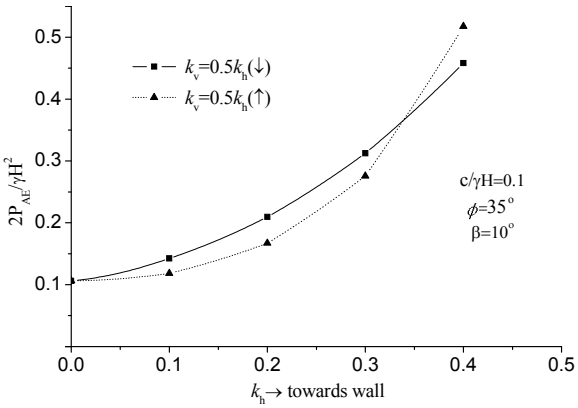

Fig. 4 Calculated P_{AE} values under downward and upward seismic inertia forces

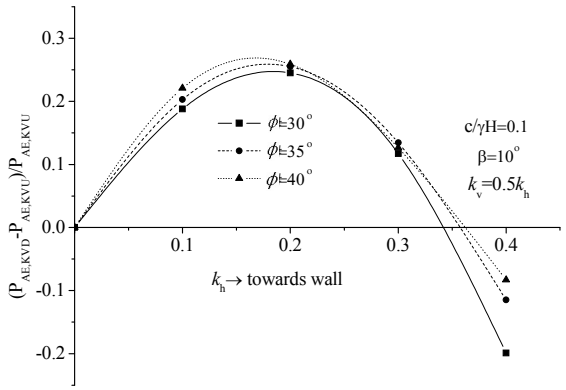

Fig. 5 Difference of P_{AE} at different soil friction angle of ϕ

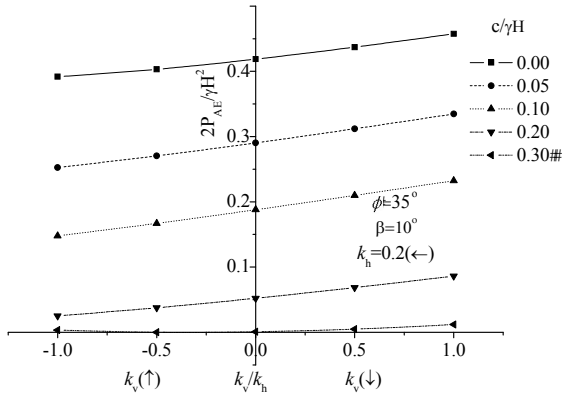

Fig. 6 Variation of active force (P_{AE}) with seismic coefficient ratio (k_v/k_h) at different dimensionless cohesion

In the design of retaining structures subjected to seismic loading, the vertical acceleration is generally taken as half of the corresponding horizontal acceleration according to most earthquake records (Fang and Chen 1995, Ling and Leshchinsky 1998, Shukla *et al*. 2009). Fig. 4 shows the difference in the dimensionless active thrust P_{ae} calculated under upward and downward vertical accelerations with different horizontal seismic accelerations. The value of P_{ae}, calculated under a downward seismic acceleration was higher than that under an upward seismic acceleration when the horizontal seismic acceleration was less than 0.35 g. However, a different conclusion can be made when the horizontal seismic acceleration was larger than 0.35g, i.e., P_{ae} calculated under a downward seismic acceleration was lower than that under an upward seismic acceleration.

Fig. 5 shows the difference in dimensionless active thrust P_{ae} determined by the vertically downward and upward seismic accelerations for soil backfills with friction angles of 30 to 40°. The subscripts KVD and KVU indicate that k_v acted downwards and upwards respectively. The

maximum difference in the calculated seismic active thrust under upward and downward seismic inertia forces reached 25%. Fig. 5 also shows that the upward seismic acceleration resulted in a higher P_{ae} when k_h exceeded 0.35. In fact, an earthquake with a horizontal acceleration greater than 0.35g is not very common (Fang and Chen 1995, Ling and Leshchinsky 1998). However, a correct acceleration direction should be chosen to ensure the safety of designed retaining structures located within a seismic active zone.

At various dimensionless cohesion $c/\gamma H$, friction anlges ϕ of soils, and slope angles β, and a given horizontal seismic inertia force towards the wall (k_h = 0.2), the relationships between the seismic active force P_{ae} and the seismic coefficient ratio k_v/k_h, were established and are shown in Figs. 6 to 8. Figs. 6 to 8 show that the active forces increased linearly with the increase of the seismic coefficient ratio from –1.0 to +1.0, regardless of the direction of the vertical seismic inertia force. Figs. 6 and 7 shows that a higher seismic active force was obtained when the vertical seismic inertia force acted downwards no matter whether the soil properties, such as dimensionless cohesion $c/\gamma H$, friction angle ϕ, and slope angle β changed. Under the given horizontal and vertical seismic inertia forces, the seismic active force P_{ae} increased with the increase of the slope angle β (Fig. 8) while it decreased with the increase of the dimensionless cohesion $c/\gamma H$ (Fig. 6) or the soil friction angle ϕ (Fig. 7).

The critical depth z_c of a tension crack behind the wall can be computed using Eq. (7). Fig. 9 shows the relationship between the relative critical depth z_c/H and the horizontal seismic acceleration coefficient k_h (towards the wall) under an upward or downward seismic inertia force. It is shown that the relative critical depth z_c/H decreased with the increase of the horizontal seismic coefficients k_h. At the given soil properties and the horizontal seismic coefficient, a greater critical depth of the tension crack was observed under an upward seismic inertia force. Fig. 10 shows the curves of relative critical depth z_c/H and dimensionless cohesion $c/\gamma H$ at the given soil properties and the horizontal and vertical seismic inertia forces. It is shown that the relative critical depth z_c/H increased linearly with the increase of the dimensionless cohesion $c/\gamma H$. Fig. 11 shows the nonlinear decrease of the active force with the cohesion.

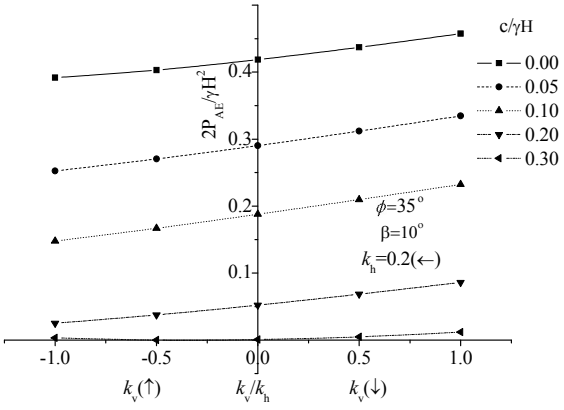

Fig. 7 Variation of active force (P_{AE}) with seismic coefficient ratio (k_v/k_h) at different soil friction angle ϕ

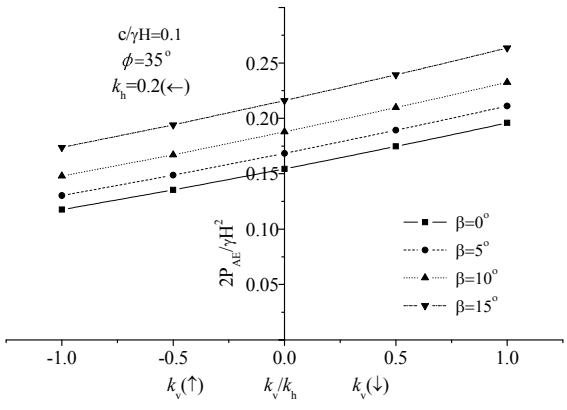

Fig. 8 Variation of active force (P_{ae}) with seismic coefficient ratio (k_v/k_h) at different slope angle β

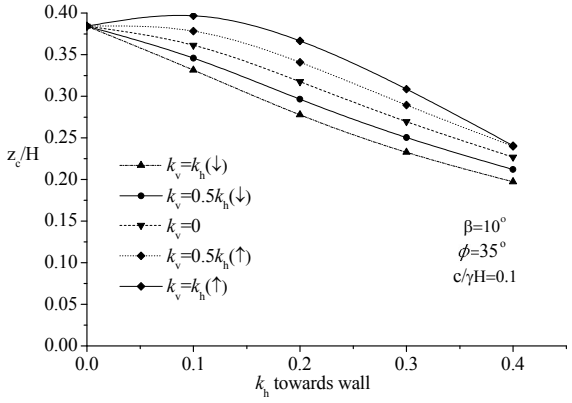

Fig. 9 Variation of critical depth (z_c/H) with horizontal seismic coefficient (k_h) under upward or downward inertia force (k_v)

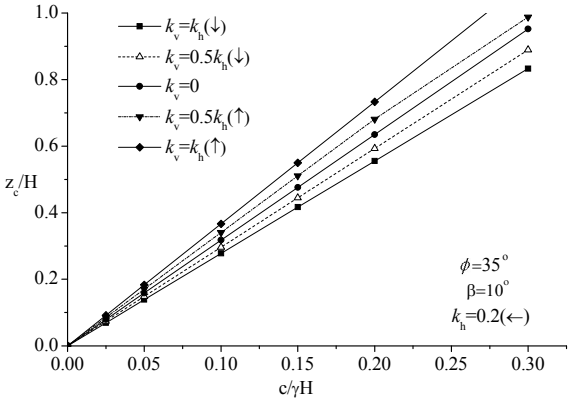

Fig. 10 Variation of relative critical depth (z_c/H) with dimensionless cohesion $c/\gamma H$ under horizontal and vertical inertia forces

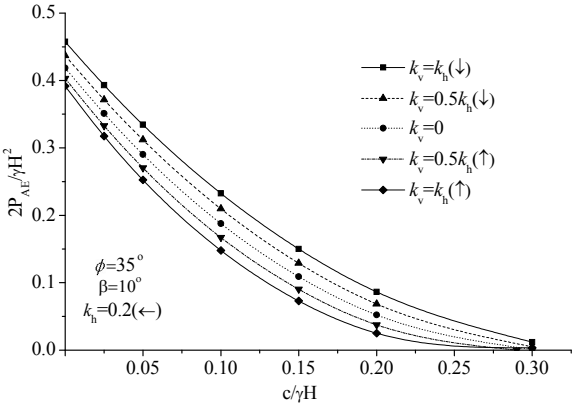

Fig. 11 Variation of active force (P_{ae}) with $c/\gamma H$ under horizontal and vertical inertia forces

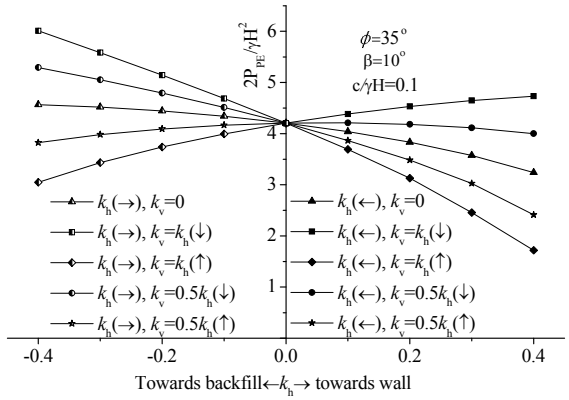

Fig. 12 Influence of seismic inertia force directions on passive resistance

5. Parametric study under seismic passive condition

Fig. 2 (b) shows a trapezoid seismic passive earth pressure distribution. The seismic passive force P_{pe} acting on the rigid retaining wall per unit length can be expressed below by combining Eqs. (3) and (4)

$$\begin{aligned} P_{\mathrm{pe}} &= \frac{1}{2}\left[\sigma_{\mathrm{pe}}\big|_{z=0} + \sigma_{\mathrm{pe}}\big|_{z=H}\right]H = \frac{1}{2}\left[K_{\mathrm{pe}}\big|_{z=H}(1 \pm k_{\mathrm{v}})\gamma H + 2c\frac{\sin\phi + 1}{\cos\phi}\cos\beta\right]H \\ &= \frac{1}{2}K_{\mathrm{pe}}\big|_{z=H}(1 \pm k_{\mathrm{v}})\gamma H^2 + cH\frac{\sin\phi + 1}{\cos\phi}\cos\beta \end{aligned} \tag{10}$$

The above equation can be expressed in a dimensionless form as follows

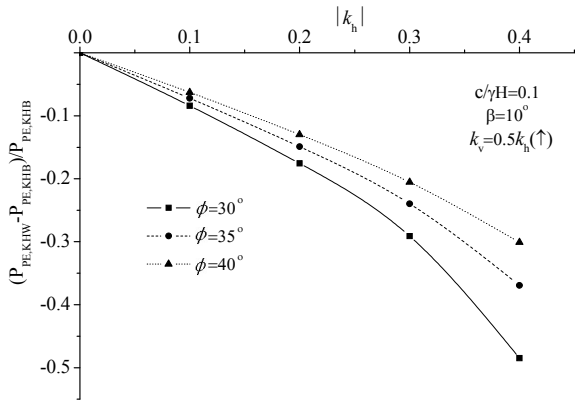

Fig. 13 Difference of P_{PE} at different friction angle of ϕ using the proposed and conventional methods

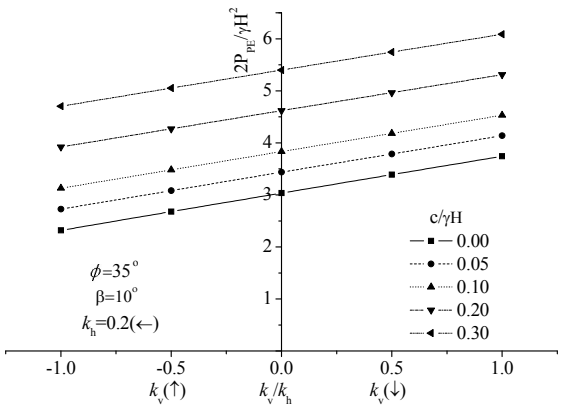

Fig. 14 Variation of passive force (P_{pe}) with seismic coefficient ratio (k_v/k_h) at different dimensionless cohesion

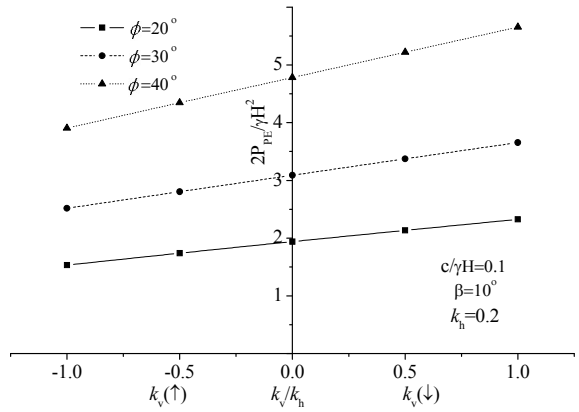

Fig. 15 Variation of passive force (P_{pe}) with seismic coefficient ratio (k_v/k_h) at different friction angle ϕ

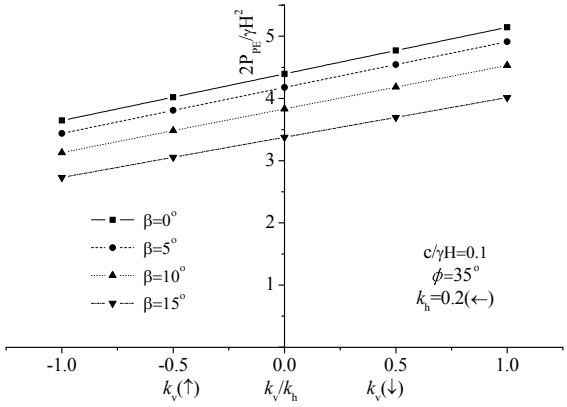

Fig. 16 Variation of passive force (P_{pe}) with seismic coefficient ratio (k_v/k_h) at different slope angle β

$$\overline{P_{\mathrm{pe}}} = P_{\mathrm{pe}}/(\tfrac{1}{2}\gamma H^2) = K_{\mathrm{pe}}\big|_{z=H}(1 \pm k_{\mathrm{v}}) + 2\frac{c}{\gamma H}\frac{1+\sin\phi}{\cos\phi}\cos\beta \tag{11}$$

To investigate the influence of the seismic acceleration directions on the seismic passive forces, the material parameters and seismic parameters shown in Table 1 were adopted with Eq. (11). A series of dimensionless seismic passive forces were obtained and are shown in Fig. 12 by changing the directions of horizontal (towards the wall or backfill) and vertical (upwards or downwards) seismic inertia forces. From a practical viewpoint, the minimum passive force should be determined for resisting the failure of a retaining structure. Fig. 12 shows that a minimum passive force P_{pe} was caused by the upward and towards-the-wall inertia forces based on the solution

proposed in this study. This result is different from Kapila's finding that the critical inertia forces acted upwards and towards the backfill using the conventional passive force equation (Kapila 1962). The differences in the calculated dimensionless passive resistance P_{pe} using the present and conventional (i.e., by Kapila in 1962) methods for the soil friction angles ϕ ranging from 30° to 40° are shown in Fig. 13. The subscripts KHW and KHB denote the inertia forces with k_h acting towards the wall in the present method and the backfill in the conventional method respectively. The maximum difference in the seismic passive resistance between the toward-the-wall and toward-the-backfill seismic inertia forces was approximately 50%. Fig. 13 also shows that the difference became greater when the horizontal seismic coefficient increased.

Figs. 14 to 16 show the relationships between the seismic passive force P_{pe} and the seismic coefficient ratio k_v/k_h at a given horizontal seismic inertia force towards the wall (k_h = 0.2) but at different dimensionless cohesion $c/\gamma H$, friction angle ϕ and slope angle β. It is shown that at a given horizontal seismic inertia force towards the wall, the passive force increased linearly with the increase of the seismic coefficient ratio from –1.0 to +1.0, regardless of the direction of the vertical seismic inertia force. Moreover, the lower seismic passive force was obtained when the vertical seismic inertia force acted upwards, irrespective of the change of the parameters such as $c/\gamma H$ (Fig. 14), ϕ (Fig. 15), and β (Fig. 16). At the given horizontal and vertical seismic inertia forces, the passive force P_{pe} decreased with the increase of the slope angleβ (Fig. 16) while that increased with the increase of the dimensionless cohesion $c/\gamma H$ (Fig. 14) or friction angle ϕ (Fig. 15).

6. Discussions

Several analytical approaches are frequently used in current practice to calculate the seismic or dynamic earth pressures/forces on retaining structures, such as the elastic theory (Wood, 1973), Coulomb's sliding wedge theory (Mononobe 1924, Okabe 1924, Seed and Whitman 1970) and Rankine's limit stress state theory (Terzaghi 1943, Richards and Shi 1994). However, there exist some significant differences in the solutions from different methods because these methods are used for specific applications in the design of retaining structures subjected to seismic excitation. For example, Wood (1973) assumed a linear elastic behavior of the wall-soil. Compared with the linearly elastic assumption made by Wood (1973), the commonly used Mononobe-Okabe method based on Coulomb's sliding wedge theory employs the assumption of sufficiently large wall deformations to induce a fully plastic stress condition in the soil, while the limit stress state approach based on Rankine's earth pressure theory allows a tensile crack at the top of the wall. In order to illustrate the differences in the several seismic earth pressure/force approaches, a typical rigid retaining structure under a horizontal seismic acceleration with a_h = 0.15 g is employed, and the wall is assumed to be vertical and smooth, while the fill consists of sandy soils with c = 0, ϕ = 36°and υ = 0.3. Comparison of the solutions from different methods are shown in Figs. 17 and 18, respectively, in which the parameter ΔP_{ae} represents the active wall force increment due to horizontal earthquake loading, and the other parameters are defined earlier.

It can be shown from Fig. 17 that the results from the improved Rankine's earth pressure theory proposed in this paper fall in between those based on Coulomb's earth pressure theory such as the Mononobe-Okabe and Seed-Whitman approaches. Moreover, the seismic force increments in this study are generally close to those by the Mononobe-Okabe approach under a high friction angle, and tend to close to those by the Seed-Whitman approach under a low friction angle. Particularly,

the results from the present study and Coulomb's sliding wedge concept are far lower than those

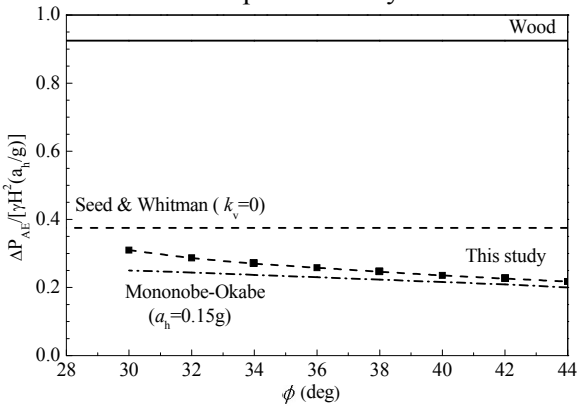

Fig. 17 Variation of seismic force increments with friction angle at a_h = 0.15 g

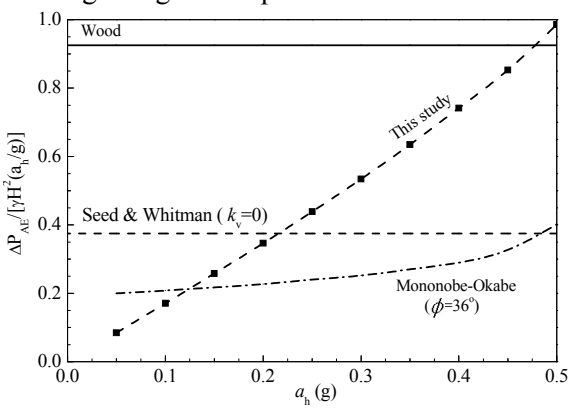

Fig. 18 Variation of seismic force increments with horizontal seismic accelerations at ϕ = 36°

from Wood's solution.

Fig. 18 shows that the results in this study are generally closer to those by the Mononobe-Okabe and Seed-Whitman approaches under low-moderate horizontal seismic accelerations, while they are close to those by Wood's elastic theory under a high horizontal seismic acceleration. That is to say, the proposed approach has a wide application for different horizontal seismic acceleration coefficients. According to the fact that very limited wall failures were observed during strong earthquakes, thus the seismic force increments from Wood's elastic theory are remarkably higher than the practical values that the retaining structures undergo. Therefore, care is required in selecting the most appropriate method to calculate the seismic forces on retaining structures under a particular seismic situation.

7. Conclusions

Based on the development of the theoretical solution and the discussion on the influence factors on seismic active and passive forces on retaining structures under seismic loading, the following conclusions can be made:

- The present study developed an analytical solution for the active and passive forces on a rigid retaining structure with c-ϕ backfill and an infinite top slope considering both the horizontal (towards the wall or the backfill) and vertical (upwards or downwards) seismic inertia forces based on Rankine's earth pressure theory and the Mohr-Coulomb yield criterion.
- For a retaining structure with c-ϕ backfill under a seismic active condition, the critical inertia forces to cause a maximum active thrust P_{ae} should act downwards and towards the wall when the horizontal seismic acceleration is less than 0.35 g. When the horizontal seismic acceleration is larger than 0.35 g, however, the critical inertia forces to cause a maximum active thrust P_{ae} should act upwards and towards the wall. Therefore, it is important to evaluate the vertical seismic inertia force in a correct direction during the

design of a retaining structure under seismic loading.

- For a retaining structure under a seismic passive condition, the critical inertia forces to cause a minimum passive resistance P_{pe} should act upwards and towards the wall.
- When only a horizontal seismic inertia force is considered in the design of a retaining structure, it is also true that the inertia force towards the wall causes a higher active thrust or a lower passive resistance than that towards the backfill.
- A tension crack is found behind the retaining structure with a c-ϕ backfill under seismic loading. A greater critical depth of the tension crack is observed under an upward seismic inertia force. The relative critical depth z_c/H decreases linearly with the increase of the horizontal seismic inertia force and increases with the increase of the dimensionless cohesion $c/\gamma H$ and thus leading to the decrease of the active force.

Acknowledgments

The authors wish to acknowledge the support of the National Natural Science Foundation of China (Grant No.51179022) and the Open Research Fund of the State Key Laboratory of Geohazard Prevention and Geoenvironmental Protection, Chengdu University of Technology (Grant No. SKLGP2010K005) for this research. In addition, the authors appreciate the anonymous reviewers for their helpful comments, which have helped the quality of the paper.

References

Budhu, M. and Al-Karni, A.V. (1993), "Seismic bearing capacity of soils", *Geotechnique*, **43**(1), 181-187.

Chen, W.F. (2007), *Limit Analysis and Soil Plasticity*, J. Ross Publishing, Fort Lauderdale, FL, USA.

Choudhury, D. and Nimbalkar, S. (2005), "Seismic passive resistance by pseudo-dynamic method", *Geotechnique*, **55**(9), 699-702.

Das, B.M. (2008), *Fundamentals of Geotechnical Engineering*, (3rd Edition), Cengage Learning, Stanford, CA, USA.

Fang, Y.S. and Chen, T.J. (1995), "Modification of Mononobe-Okabe theory", *Geotechnique*, **45**(1), 165-167.

Ghosh, P. (2008), "Seismic active earth pressure behind a nonvertical retaining wall using pseudo-dynamic analysis", *Can. Geotech. J.*, **45**(7), 117-123.

Gnanapragasam, N. (2000), "Active earth pressure in cohesive soils with an inclined ground surface", *Can. Geotech. J.*, **37**(2), 171-177.

Kapila, J.P. (1962), "Earthquake resistant design of retaining walls", *Proceedings of the Second Earthquake Symposium*, Roorkee, India, December.

Lancellotta, R. (2002), "Analytical solution of passive earth pressure", *Geotechnique*, **52**(8), 617-619.

Lancellotta, R. (2007), "Lower-bound approach for seismic passive earth resistance", *Geotechnique*, **57**(3), 319-321.

Ling, H.I. and Leshchinsky, D. (1998), "Effects of vertical acceleration on seismic design of geosynthetic-reinforced soil structures", *Geotechnique*, **48**(3), 347-373.

Mononobe, N. (1924), "Consideration into earthquake vibrations and vibration theories", *J. Japan. Soc. Civil Eng.*, **10**(5), 1063-1094.

Nian, T.K. and Han, J. (2013), "Analytical solution for seismic earth pressures in c-φ soil with an infinite slope", Technical Note, *ASCE J. Geotech. Geoenviron. Eng.*, **139**(9), 1611-1616.

Okabe, S. (1924), "General theory on earth pressure and seismic stability of retaining wall and dam", *J. Japan. Soc. Civil Eng.*, **10**(5), 1277-1323.

Richards, R. and Shi, X. (1994), "Seismic lateral pressures in soils with cohesion", *J. Geotech. Eng., ASCE*,

120(7), 1230-1251.
Richards, R., Elms, D.G. and Budhu, M. (1990), "Dynamic fluidization of soils", *J. Geotech. Eng., ASCE*, **116**(5), 740-759.
Seed, H.B. and Whitman, R.V. (1970), "Design of earth retaining structures for dynamic loads", *Proceedings of Special Conference on Lateral Stresses in the Ground and Design of Retaining Structures*, Ithaca, New York, USA, June.
Shukla, S.K. and Habibi, D. (2011), "Dynamic passive pressure from c-ϕ soil backfills", *Soil Dyn. Earthq. Eng.*, **31**(6), 845-848.
Shukla, S.K., Gupta, S.K. and Sivakugan, N. (2009), "Active earth pressure on retaining wall for c-ϕ soil backfill under seismic loading condition", *J. Geotech.Geoenviron. Eng., ASCE*, **135**(5), 690-696.
Terzaghi, K. (1943), *Theoretical Soil Mechanics*, John Wiley & Sons, Inc., New York, NY, USA.
Wood, J.H. (1973), "Earthquake-induced soil pressures on structures", Ph.D. Dissertation, California Institute of Technology, Pasadena, CA, USA.
Yao, L., Feng, J. and Yang, M. (2009), "Damage analysis of subgrade structures in Wenchuan earthquake and recommendations for improving seismic design code", *J. Southwest Jiaotong Univ.*, **44**(3), 301-311.

GC